Arch. Mech., 53, 1, pp. 23–43, Warszawa, 2001

On quantum turbulence in superfluid ^{4}He

Ł. LIPNIACKI

Polish Academy of Sciences
Institute of Fundamental Technological Research
Świętokrzyska St. 21, 00–049 Warsaw, Poland

THE ALTERNATIVE APPROACH to the homogeneous quantum turbulence is proposed in order to derive the evolution equation for vortex line-length density. Special attention is paid to reconnections of vortex lines. According to our previous paper, the summary line-length change ΔS of two vortex lines resulting from the reconnection (in the presence of counterflow V_{ns}) can be approximated by the expression: $\Delta S = -at^{1/2} + bV_{ns}^2 t^{3/2}$, with $a > 0$, $b \geq 0$. The dynamics of vortex lines in the tangle is considered as a sequence of reconnections followed by "free" evolutions. For the steady-state turbulence, the average line-length change $<\Delta S>$ between reconnections has to be zero. If, for a given value of the counterflow, the line density is smaller than the equilibrium one, the reconnections occur less frequently and $<\Delta S>$ becomes positive. As a result, the line density grows until the equilibrium is restored. On the other hand, when the line-density is too large, the reconnections are very frequent, so the lines shorten between reconnections and the line density becomes smaller. The time derivative of total line density is proportional to the reconnection frequency multiplied by the average line-length change due to a single reconnection. The evolution equation obtained in the proposed approach resembles the alternative Vinen equation.

Key Words: ^{4}He, quantum turbulence, reconnection.

1. Introduction

THE VARIETY OF THE DYNAMIC phenomena exhibited by the superfluid ^{4}He involves the appearance and motion of quantized vortices. Due to the existence of these singularities, the superfluid component is coupled dissipatively with the normal one. We recall that at low velocities, He II (superfluid ^{4}He) flows in the frictionless, presumably laminar manner consistent with the ideal fluid description. When the counterflow (the relative velocity of the components) $V_{ns} = V_n - V_s$ becomes sufficiently large, the superfluid laminar flow develops into a superfluid turbulent flow in which the quantum vortices form a chaotic tangle.

The simplest way of generating a sizable V_{ns} (SCHWARZ and ROZEN [11]) is to seal off one end of the channel and place a heater there. The normal fluid transporting the entropy flows out of the channel with average velocity

$V_n = \dot{Q}/A\rho ST$, where $\dot{Q}$ is the heat input, A is the channel cross-sectional area, ρ is the total fluid density, S is the specific entropy, and T is the temperature. The normal fluid moving away from the heater is replaced by the superfluid flowing in the opposite direction, the superfluid velocity being determined by the condition of zero net mass transport $\rho_n V_n + \rho_s V_s = 0$. Since the normal and superfluid densities ρ_n and ρ_s are known functions of temperature, V_{ns} can the be varied in a controlled way, by simply adjusting the heater input $\dot{Q}$.

The pioneering studies of superfluid turbulence were conducted by VINEN [14, 15, 16, 17], who proposed the mechanisms of vortex generation and decay. He observed that in the presence of the counterflow velocity V_{ns}, the vortex ring can blow up, and that the line-line reconnections (predicted by Feynman) can give rise to new rings. These phenomenological considerations led him to the (Vinen) equation which described the evolution of line-length density L

$$\frac{\partial L}{\partial t} = \alpha_v V_{ns} L^{3/2} - \beta_v L^2 \,, \tag{1.1}$$

where α_v and β_v are temperature-dependent coefficients which must be determined experimentally.

Since than, a considerable progress has been made and the new methodology based on careful analysis of the motion of quantized vortices using extensive numerical simulation has been developed.

SCHWARZ [10] simulated the evolution of a vortex tangle basing on an equation describing vortex motion in the localized induction approximation, and on the assumption that vortex lines reconnect when they get close enough. Schwarz defined some characteristic measures I_l, c_2 describing the vortex tangle, and in terms of these measures he interpreted the original Vinen coefficients α_v and β_v. He showed by scaling arguments that for the equilibrium turbulence, these measures do not depend on L, and evaluated them for various friction parameters α. Later SCHWARZ and ROZEN [11] analyzing, by numerical simulations, large transients when the line-length density grows from very small to very large values, concluded that the coefficients c_2 and especially I_l deviated substantially from their steady-state values. This means that despite the fact that Vinen equation can satisfactorily fit most of the experimental data, it is probably not proper, from a more theoretical point of view.

The more powerful computers allow now (NORE *et al.* [7], BARENGHI *et al.* [1]) the numerical simulations of quantum tangle basing on nonlinear Schrodinger equation (NLSE). NLSE describes the evolution of complex field $\Psi = \rho_s \exp(i\Theta)$, which is related to superfluid velocity (V_s =grad Θ) and density $\rho_s = |\Psi|$ via the Madelung transformation. The quantum vortices are traced by lines on which $\Psi = 0$.

In the present paper an alternative approach to the homogeneous quantum turbulence is proposed. The main aim is to derive the evolution equation for the vortex line-length density L in which the coefficients may be determined with the help of relatively simple simulations of evolution of single vortex lines. The paper uses the analysis of motion of quantum vortices presented in two previous papers of the author (LIPNIACKI [4, 5]). The various aspects of the vortex three-dimensional dynamics like line-line and line-boundary reconnection, pinning and depinnig, can be found in the paper by SCHWARZ [9].

The dynamics of quantum vortices will be considered in the localized induction approximation (LIA) supplemented by the assumption that when two vortex lines cross each other, they undergo a reconnection. If the curve traced out by a vortex filament is specified in the parametric form $s(\xi, t)$, the instantaneous velocity of a given point of the filament can be approximated by the equation

$$\dot{s} = \beta s' \times s'' + V_s + \alpha s' \times (V_{ns} - \beta s' \times s'') - \alpha' s' \times [s' \times (V_{ns} - \beta s' \times s'')] , \tag{1.2}$$

where the dot and prime denote instantaneous derivatives with respect to time t and arc length ξ, respectively, α and α' are the nondimensional friction coefficients, and

$$\beta = \frac{\kappa}{4\pi} \ln\left(\frac{c}{a_o <s''>}\right) \approx \kappa , \tag{1.3}$$

where κ is the quantum of circulation, c is a constant of order one, $<s''>$ is the average curvature of the vortices in the tangle, and $a_o \simeq 1.3 * 10^{-8}$ cm is the effective core radius of a quantized vortex.

The parameter α' is small and according to SCHWARZ [9] considerations confirmed by numerical analysis, the last term in Eq. (1.2) (proportional to α') can be neglected when the quantum tangle is considered. In the further analysis we also put $\alpha' = 0$.

The factor β can be absorbed into the reduced time $\tau = \beta t$ and the velocity $v_n = V_n/\beta$, $v_s = V_s/\beta$, with $v_{ns} = v_n - v_s$. Hence in the superfluid reference frame Eq. (1.2) reduces to

$$\dot{s} = s' \times s'' + \alpha s'' + \alpha s' \times v_{ns} . \tag{1.4}$$

Moreover (SCHWARZ [11]), if one takes any solution of Eq. (1.4) and multiplies it by a scale factor λ, all the velocities by λ^{-1}, and the time (times) by λ^2, one obtains another solution of this equation. Any property $P(\mathbf{r}, v, \tau, ...)$ evaluated in any particular solution of Eq. (1.4), relates to the same property $P(\lambda\mathbf{r}, v/\lambda\, \lambda^2\tau, ...)$, but evaluated on the scaled solution, according to

$$P(\lambda\mathbf{r}, v/\lambda, \lambda^2\tau, ...) = f(\lambda) P(\mathbf{r}, v, \tau, ...) , \tag{1.5}$$

where the form of $f(\lambda)$ depends on the particular combination of distances and times represented by property P. For example, the evaluation of the line-length density at some point in the vortex tangle involves measuring the length of quantized vortex line contained in some sampling volume and dividing by the sampling volume. These scale as λ and λ^3, respectively, so that $f(\lambda) = \lambda^{-2}$ for the line-length density L:

$$L(\lambda \mathbf{r}, v_{ns}/\lambda, \lambda^2 \tau) = \lambda^{-2} L(\mathbf{r}, v_{ns}, \tau) \ . \tag{1.6}$$

Hence for the steady-state turbulence, when the line density depends only on v_{ns} one gets from Eq. (1.6)

$$L \sim v_{ns}^2 \ . \tag{1.7}$$

Let us note that the given line-length density determines the characteristic space scale l_o

$$l_o = L^{-1/2} \ . \tag{1.8}$$

The length l_o plays an important role in the analysis of the turbulence. First, the quantities like average spacing between vortices or the characteristic radius of curvature $<|s''|>$ of lines in the tangle, scale as $L^{-1/2}$ and are of order l_o. The length l_o gives also the minimal scale below which the macroscopic description of vortex tangle loses its sense.

If the motion of vortex filament fulfills Eq. (1.4), its line-length $l = \int d\xi$ satisfies the equation (SCHWARZ [9])

$$\frac{\partial l}{\partial \tau} = \int \left(\alpha v_{ns} \cdot (s' \times s'') - \alpha |s''|^2 \right) d\xi \ . \tag{1.9}$$

The first term of the above equation describes the influence of the counterflow velocity onto the line-length. This term can be positive or negative, depending on the angle between the binormal $(s' \times s'')$ and the counterflow. It is obvious that when the totally isotropic vortex tangle is considered, the first term has to average zero. This means that in the steady-state the vortex tangle cannot be totally isotropic since some directional anisotropy of the binormal is needed to balance the second term, which is always negative.

In the presented model, special attention will be paid to reconnections of vortex lines (Fig. 1). To see why the reconnections play the crucial role in the quantum turbulence, let us consider the evolution of a single circular vortex ring subject to the counterflow v_{ns}. Let $\Theta(t)$ be the relative angle between the counterflow v_{ns} and the vortex binormal. It can be shown (LIPNIACKI [4]) that if initial ring radius R_i and $\Theta_i = \Theta(0)$ satisfy the inequality

$$R_i > R_o(\Theta_i) = \frac{\Theta_i}{v_{ns} \sin \Theta_i} \ , \tag{1.10}$$

then the ring will blow up and die on the boundaries, and if $R_i < R_o(\Theta_i)$, the ring will contract to a point. The picture is not very different when instead of rings, one considers ovals. This simple example shows that to sustain turbulence, the reconnections are needed to produce new kinks which can develop into new loops.

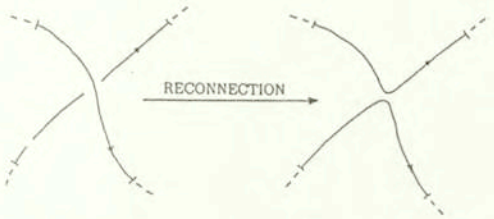

FIG. 1. Collision-reconnection of two vortex segments.

2. The model

Let us recall (LIPNIACKI [5]) some facts concerning the specific behavior of quantum vortices after reconnection. Immediately after each reconnection, both resulting lines have very big curvature (close to the reconnection point), the second term of Eq. (1.9) prevails and the lines shortens. Note also that just after the reconnection, close to the reconnection point, the two vortices have the binormals of opposite directions. During further evolution the characteristic curvatures get smaller, and also the two vortices turn so that the average value of $v_{ns} \cdot (s' \times s'')$ becomes positive. As a result, the total length of vortices starts growing. The anisotropy of the distribution of the binormal results from the "action" of the counterflow. In the idealized reconnection of two straight vortices, the summary line-length change $\Delta S(\tau)$ of two vortices resulting from the reconnection can be satisfactorily approximated in the following form:

$$\Delta S(\tau) = -a\,\tau^{1/2} + b\,\tau^{3/2} v_{ns}^2 \,, \tag{2.1}$$

where $a > 0$, $b \geq 0$ are the nondimesional coefficients dependent on friction coefficient α and the specific reconnection configuration (the relative angle between reconnecting lines and the counterflow velocity v_{ns}).

If the vortex tangle is considered as a whole, more important is the average line-length change $<\Delta S(\tau)>$ of lines resulting from reconnection. The function $<\Delta S(\tau)>$ has the same form as $\Delta S(\tau)$ and its parameters $<a>$, $<b>$ have been estimated (for isotropic tangle) in the previous paper (LIPNIACKI [5]); we will recall this result later. For steady-state turbulence, the average line-length change between reconnections has to be zero. If for the same value of the counterflow v_{ns} the line density is smaller, the reconnections occur less frequently, and so, the

characteristic time between reconnections is longer and according to Eq. (2.1), the line-length change between reconnections becomes positive. As a result, the line density of vortex tangle grows until the equilibrium is restored. Inversely, when the line-length density is too large, the reconnections are more frequent so that the decaying term in Eq. (2.1) prevails and the line density gets smaller. The model of quantum turbulence we will construct below, bases on the presented mechanisms which explains how the equilibrium density of vortex tangle can be sustained and restored.

We concentrate on the quasi-isotropic turbulence (i.e. with net macroscopic superfluid vorticity equal to zero), derive the evolution equation for line-length density. Later, after some discussion and comparison of the obtained results with those of the Vinen-Schwarz theory, we signal how the model may be generalized in the case in which the considerable macroscopic vorticity is present.

In the quasi-isotropic case we assume (constructing the model) that directional distribution of vortex lines is uniform, i.e. we assume that the unit vector s' is distributed uniformly over the unit sphere. Next we find that such assumption cannot be strictly valid; some directional anisotropy of vortex tangle results from the action of the counterflow V_{ns}. Moreover, the nonuniform distribution of the binormal is needed just to sustain the vortex tangle. The assumption of uniform directional distribution should be understood as the zero order approximation, while the anisotropy resulting from the model is the first order perturbation.

The plan of our considerations is the following; first we estimate the average velocity v_o of vortex lines. This will be used to calculate the reconnections frequency f_r, and the characteristic time spacing τ_c between reconnections. Then the average line-length change due to a single reconnection will be found as $<\Delta S(\tau_c)>$. Having the reconnection frequency and length change due to single reconnection, we will obtain the time derivative of line-length density.

2.1. The average line velocity $v_o = <|\dot{s}|>$

Let us note that all three terms of Eq. (1.4) lie in the plane which is perpendicular to the local tangent s' to the vortex line. Besides, the first two terms are perpendicular to each other, $|s'| = 1$, hence

$$v_{12} := |s' \times s'' + \alpha s''| = |s''|\sqrt{1+\alpha^2}\ . \tag{2.2}$$

The mean square value of the third term of Eq. (1.4) (under the assumption that the distribution of s' is isotropic) is

$$<|s' \times v_{ns}|^2> = \frac{(\alpha v_{ns})^2}{4\pi} \int_0^{\pi} \int_0^{2\pi} \sin^3(\Theta_j)\, d\Theta_j\, d\phi_j = \frac{2}{3}(\alpha v_{ns})^2\ . \tag{2.3}$$

Hence v_o^2 reads:

$$v_i^2 = <|s''|^2> (1+\alpha^2) + \frac{2}{3}(\alpha v_{ns})^2 + <(s' \times s'' + \alpha s'')(\alpha s' \times v_{ns})> . \tag{2.4}$$

We assume (in the zero order approximation) that for given s', both s'' and $-s''$ are equally probable i.e that the sign of curvature is not correlated with the tangent to the vortex. This means that the last term of Eq. (2.4) vanishes, and as a result

$$v_o = \sqrt{<|s''|^2> (1+\alpha^2) + \frac{2}{3}(\alpha v_{ns})^2} . \tag{2.5}$$

Assuming that $|s''| = 1/l_o = L^{1/2}$ we get finally the estimate of the mean square value of vortices velocity v_o in the form

$$v_o = \sqrt{L(1+\alpha^2) + \frac{2}{3}(\alpha v_{ns})^2} . \tag{2.6}$$

2.2. The total reconnection frequency (number of reconnections per time and unit volume)

Let us divide the vortex lines into segments of length l_o which is equal to average value of the radius of lines curvature, and characteristic spacing between vortex lines forming the tangle. Because the length l_o is equal to spacing between the lines, we may expect that each segment moves (more or less) as a unity, but the motions of the neighboring segments are not strongly correlated. Moreover, because the length of segments are equal to the characteristic radius of curvature, when considering the collisions, the segments can be roughly treated as straight ones. We will assume that every collision of vortex segments leads to a reconnection; such assumption is well justified by numerical simulations (SCHWARZ [9]). For the sake of simplicity we assume that all the segments move with the same speed v_o.

Consider now the collision of two segments parallel to unit vectors e^i, e^j. Let us asign the reference frame to the first unit vector. Let $R_{i,j}$ be the rhombus with center placed in the center of the first segment, and sides (having length l_o) parallel to e^i, e^j.

When the center of the second segment goes through $R_{i,j}$, then the two segments come into collision (Fig. 2). The oriented area $\mathbf{S}_{i,j}$ of rhombus $R_{i,j}$, called from now on the "collision surface", is

$$\mathbf{S}_{i,j} = (l_o)^2 e^i \times e^j . \tag{2.7}$$

The collision frequency $f_{i,j}$ of the given segment parallel to e^i and moving with velocty v_i, with other segments parallel to e^j and moving with velocity v_j, is

$$f_{i,j} = n_j \mathbf{S}_{i,j} \cdot (v_i - v_j) , \tag{2.8}$$

where n_j denotes the density of segments parallel to e_j and moving with velocity v_j. Let Θ_i, Θ_j denote the angles between normal to $\mathbf{S}_{i,j}$ and velocities v_i, v_j, respectively, then

$$f_{i,j} = n_j v_o l_o^2 |e^i \times e^j| |\cos(\Theta_i) - \cos(\Theta_j)| \,. \tag{2.9}$$

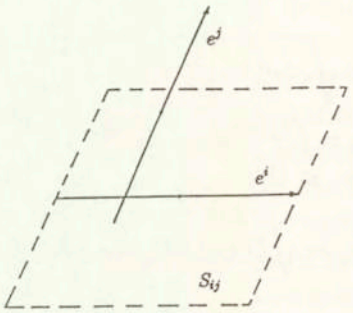

FIG. 2. Collision surface $\mathbf{S}_{i,j}$, corresponding to the collision of two vortex segments which have length l_o, and are parallel to $\mathbf{e}^i$, $\mathbf{e}^j$.

Hence the average collision frequency for a segment (of length l_o) is

$$f(l_o) = n v_o l_o^2 \, <|e^i \times e^j| |\cos(\Theta_i) - \cos(\Theta_j)|> \,, \tag{2.10}$$

where $<>$ means averaging over the directions e^i, e^j and angles $\Theta_i \in (0, \pi)$, $\Theta_j \in (0, \pi)$, and $n = L/l_o$ is the total segment density. Let us note that because unit vectors e^i, e^j are uncorrelated with Θ^i, Θ^j, one can average $|\mathbf{S}_{i,j}|$ and $|\cos(\Theta_i) - \cos(\Theta_j)|$ separately. Calculating the average collision surface σ_o one can, without any loss of generality, assume that e^i is parallel to the $\hat{z}$ axis. Then

$$\sigma_o = <|\mathbf{S}_{i,j}|> = \frac{(l_o)^2}{4\pi} \int_0^{\pi} \int_0^{2\pi} \sin(\Theta_j)^2 \, d\Theta_j \, d\phi_j = \frac{\pi}{4} l_o^2 \,, \tag{2.11}$$

while

$$<|\cos(\Theta_i) - \cos(\Theta_j)|> = \frac{1}{\pi^2} \int_0^{\pi} \int_0^{\pi} |\cos(\Theta_i) - \cos(\Theta_j)| \, d\Theta_i \, d\Theta_j = \frac{8}{\pi^2} \,. \tag{2.12}$$

Finally from Eq. (2.10)

$$f(l_o) = \sigma_o \, <|\cos(\Theta_i) - \cos(\Theta_j)|> n v_o = \frac{2}{\pi} l_o v_o L \tag{2.13}$$

since $n = L/l_o$.

In fact, such a calculated reconnection frequency is probably underestimated due to the following reasons.

(1) According to SCHWARZ [9] numerical considerations, the reconnection is initiated by nonlocal interactions when the spacing between lines is smaller than $\Delta \approx 2R/\ln(R/a_o)$, where R is the radius of curvature and $a_o = 1.3\ 10^{-8}$ cm is the vortex core radius. The typical tangle density is $L \sim 10^4 \div 10^6/\mathrm{cm}^2$, what corresponds to $R \sim 10^{-2} \div 10^{-3}$cm, so $\Delta \approx R/5 \approx l_o/5$. This means that even if $\Theta_1 = \Theta_2$ or $S_{i,j} = 0$, the reconnection may take place if only the passing distance is smaller than $l_o/5$. Because of a very complicated nature of nonlocal interactions it is very difficult to analyze the effect of additional collisions quantitatively. For example, two antiparallel vortices reconnect when passing close enough, being parallel do not. Probably the best way to take into account those additional reconnections is to enlarge the collision surface by $l_o^2/5$ or just the reconnection frequency by $l_o v_o L/5$.

(2) The assumption that all the vortex segments move with the same speed reduce the average relative velocity of segments, and the reconnection frequency $f(l_o)$.

Taking into account points (1), (2) we have

$$f(l_o) = c l_o v_o L \ . \tag{2.14}$$

where c is close to unity.

Hence, the total reconnection frequency (per unit volume) f_r is equal to

$$f_r = \frac{n f(l_o)}{2} = \frac{c v_o L^2}{2} \ . \tag{2.15}$$

The factor $1/2$ results from the fact that in each reconnection two segments are involved.

The lines resulting from reconnection are sharply bent close to the reconnection point where the characteristic curvature is much greater than the average curvature of the vortex lines forming a tangle. In our considerations we neglect the lines curvature at the moment prior to reconnection and use the results of the previous paper (LIPNIACKI [5]), where the reconnection of straight vortex filaments has been analyzed. Such approximation seems reasonable until the characteristic curvature caused be the reconnection is greater than the average curvature in a vortex tangle, or (what in fact means the same) until the length of reconnection disturbance is smaller than l_o. Fortunately, the average time $\tau_c(l_o)$ after which the segment of length $l_o = L^{-1/2}$ will come into next collision is

$$\tau_c(l_o) = \frac{1}{f(l_o)} = \frac{1}{c L^{1/2} v_o} = \frac{l_o}{c v_o} \ , \tag{2.16}$$

while time $\tau_o(l_o)$ in which the disturbance caused by reconnection grows to the size of order l_o is (LIPNIACKI [4])

$$\tau_o(l_o) = l_o^2 \,. \tag{2.17}$$

Because

$$v_o = \sqrt{(1+\alpha^2)L + \frac{2}{3}(\alpha v_{ns})^2} \approx L^{1/2} \approx l_o^{-1}, \tag{2.18}$$

these two times are roughly equal. This means that the evolution of line segment of length l_o looks as follows: reconnection – evolution during which the reconnection disturbance grows (roughly) up to the size of the segment – next reconnection. Of course after each reconnection the segment loses its identity.

According to the above, the line-length change caused by each reconnection will be approximated by the line-length change of straight reconnecting lines $\Delta S(\tau_c)$, where

$$\tau_c(l_o) = \frac{1}{cL^{1/2}v_o} \,. \tag{2.19}$$

Hence the time derivative of line-length density L reads

$$\frac{dL}{d\tau} = f_r \; <\Delta S(\tau_c)> \;, \tag{2.20}$$

where (recall) f_r is the total reconnection frequency and $< \Delta S(\tau_c) >$ is the average line-length change due to the single reconnection. According to Eq. (2.1), the average line-length change reads:

$$<\Delta S(\tau_c)> = - <a(\alpha)> \; \tau^{1/2} + <b(\alpha)> \; \tau^{3/2} v_{ns}^2 \,, \tag{2.21}$$

where $<\quad>$ denotes the averaging over all reconnection configurations (which are described by directional vectors of reconnecting lines in the direction of counterflow velocity v_{ns}).

Putting $<\Delta S(\tau_c)>$ from Eq. (2.21) with τ_c from Eq. (2.19) and f_r from Eq. (2.15) into Eq. (2.20), we get finally

$$\frac{dL}{d\tau} = \frac{1}{2}\Big(- c^{1/2} <a(\alpha)> \; L^{7/4} \, v_o^{1/2} + c^{-1/2} <b(\alpha)> \; L^{5/4} \, v_o^{-1/2} \, v_{ns}^2 \Big) \,, \tag{2.22}$$

with

$$v_o = \sqrt{<|s''|^2> (1+\alpha^2) + \frac{2}{3}(\alpha v_{ns})^2} \,. \tag{2.23}$$

The nondimensional coefficients $<a(\alpha)>$, $<b(\alpha)>$ have been estimated in the previous paper (LIPNIACKI [5]) with the help of numerical simulations, and in the following section we will recall these results.

3. Numerical estimations

To determine the average line-length change $<\Delta S(\tau)>$ of lines $\Delta S(\tau)$ resulting from reconnection, one should average over all reconnection configurations with respect to the direction of counterflow. Numerically it is rather impossible, hence to estimate $<\Delta S(\tau)>$ it was assumed that all lines in the tangle are parallel or antiparallel to 3 directions: $\hat{x}, \hat{y}, \hat{z}$, while the direction of counterflow is $(1,1,0)$. Let us note that such assumption may be only adequate for quasi isotropic case. For anisotropic case other representation should be used. The accuracy of the above method may be augmented by taking more directions into account.

The numerical simulations for the equation

$$\dot{s} = s' \times s'' + \alpha s'' + \alpha s' \times v_{ns} \tag{3.1}$$

were carried for $\alpha = 0.1$. The best fit for $\Delta S_o =< \Delta S >$ in the form (discussed previously)

$$\Delta S_o = - <a(\alpha)> \tau^{1/2} + <b(\alpha)> \tau^{3/2} v_{ns}^2 \tag{3.2}$$

was found for $a = 0.710$, $b = 0.0138$. The characteristic nondimensional time $\tau_o v_{ns}^2$ after which $\Delta S_o = 0$ is $\tau\, v_{ns}^2 = a/b = 51.2$. The time τ_o plays an important role in the analysis of turbulence, because in the equilibrium state τ_o and τ_c – characteristic times between reconnection should be equal.

To estimate the average line-length change for different α, we note that neglecting the first term of Eq. (3.1) i.e. the self-induction and using the simplified dynamic equation in the form

$$\dot{s} = \alpha s'' + \alpha s' \times v_{ns} \ , \tag{3.3}$$

one gets roughly the same rate of line change, when averaging over representative sample of reconnection configurations. This is due to the fact (see LIPNIACKI [5] for more details) that the first term in Eq. (3.1) pushes the vortex along local binormal which does not change the vortex length. Indeed (for $\alpha = 0.1$) the characteristic time of zero line-length change obtained in the simulations without self-induction is 45.7, so it is only 12% smaller when calculated with the use of the full dynamic equation. The use of the simplified dynamic equation has such an advantage that now the coefficient α can be absorbed into time scale. Hence

Eq. (3.2) can be transformed into

$$\Delta S_o = - <a(\alpha)> \tau^{1/2} + <b(\alpha)> \tau^{3/2} v_{ns}^2 = -a_o(\alpha\tau)^{1/2} + b_o(\alpha\tau)^{3/2} v_{ns}^2 , \tag{3.4}$$

what implies

$$<a(\alpha)> = a_o \alpha^{1/2} , \quad <b(\alpha)> = b_o \alpha^{3/2}, \tag{3.5}$$

with numerically calculated $a_o = 2.34$, $b_o = 0.514$. Let $A = a_o/2 = 1.17$, $B = b_o/2 = 0.257$. Then from Eqs. (2.22), (3.5) one gets

$$\frac{dL}{d\tau} = -c^{1/2} A \alpha^{1/2} L^{7/4} v_o^{1/2} + c^{-1/2} B \alpha^{3/2} L^{5/4} v_o^{-1/2} v_{ns}^2 . \tag{3.6}$$

Now we set $c = 1$ to get estimated but concrete coefficients in final form of the evolution equation; in primary variables $t = \tau/\beta$ and $V_{ns} = \beta v_{ns}$, $V_o = \beta v_o$ we have

$$\frac{dL}{dt} = -A\beta^{1/2}\alpha^{1/2} L^{7/4} V_o^{1/2} + B\beta^{-1/2}\alpha^{3/2} L^{5/4} V_o^{-1/2} V_{ns}^2 , \tag{3.7}$$

with

$$V_o = \sqrt{\beta^2(1+\alpha^2)L + \frac{2}{3}(\alpha V_{ns})^2} . \tag{3.8}$$

The equilibrium vortex density L_∞ is given by

$$L_\infty = \frac{V_{ns}^2}{\beta^2(1+\alpha^2)} \left(\sqrt{\frac{\alpha^4}{9} + (1+\alpha^2)\left(\frac{B\alpha}{A}\right)^2} - \frac{\alpha^2}{3} \right) = w(\alpha) \left(\frac{V_{ns}}{\beta}\right)^2 . \tag{3.9}$$

When $\alpha \ll 1$ and $\alpha V_{ns} \ll \beta L$, the particle velocity can be approximated by $\tilde{V}_o = \beta L^{1/2}$ and the evolution equation simplifies to

$$\frac{dL}{dt} = -A\beta\alpha^{1/2} L^2 + B\beta^{-1}\alpha^{3/2} L V_{ns}^2 . \tag{3.10}$$

4. Results

4.1. Critical remarks

The time derivative of line-length density (Eq. (2.20))

$$\frac{dL}{d\tau} = f_r <\Delta S(\tau_c)> , \tag{4.1}$$

is expressed as a product of reconnection frequency and average line-length change due to a single reconnection. Such approach includes of course some

idealization. In real turbulence one may expect that there are line segments (of length l_o) for which the time of "free" evolution is significantly shorter or longer than the average $\tau_c(l_o)$ used to calculate ΔS. Expression (4.1) cannot be valid when considering the line density changes in times shorter than the average time spacing between reconnections $\tau_c(l_o)$ (Eq. (2.16)). This can be important when considering sharp transitions in which the value of V_{ns} grows significantly. Besides, both the reconnection frequency f_r and the average line-length change $\Delta S(\tau)$ are estimated with some errors.

1) The coefficient c appearing in the expression for reconnection frequency

$$f_r = \frac{c v_o L^2}{2} \tag{4.2}$$

has been finally replaced by unity. Fortunately, in evolution equation (3.6) coefficient c appears only as $c^{1/2}$ and $c^{-1/2}$. This means that possible input error is roughly two times smaller than the error made by replacing c by unity, and probably is not greater than 10%.

2) The possible errors in estimation of the average line-length change $<\Delta S(\tau)>$

i) The initial curvature of reconnecting lines has been neglected.

ii) The relatively small sample of reconnecting lines has been considered to calculate the average value of $\Delta S(\tau)$. The possible error is of the order of $10 \div 20\%$ (see discussion in LIPNIACKI [5]).

iii) To calculate $\Delta S(\tau)$ for $\alpha \neq 0.1$, the simplified dynamical equation has been applied; the expected error is also of the order of $10 \div 20\%$.

Keeping in mind the above remarks one cannot expect that the numerical accuracy of Eq. (3.7) will be better than 50%; what is not so bad when comparing with the experimental data which varies significantly from experiment to experiment.

4.2. The obtained evolution equation versus Schwarz and Rozen simulation and experiments

Equations (3.7), (3.10) should be confronted with other two equations describing the evolution of vortex line density, namely:

1) The classical Vinen (-Schwarz) equation

$$\frac{dL}{dt} = -\beta \alpha {c_2}^2 \, L^2 + \alpha I_l \, L^{3/2} |V_{ns}| \, , \tag{4.3}$$

with nondimensional coefficients $c_2(\alpha)$ and $I_l(\alpha)$:

$$c_2^2 = \frac{1}{\Omega L^2} \int (s'')^2 d\xi \, , \tag{4.4}$$

$$I_l \hat{V}_{ns} = \frac{1}{\Omega L^{3/2}} \int s' \times s'' d\xi \,, \tag{4.5}$$

where $\hat{V}_{ns}$ is the unit vector in the direction of V_{ns} and Ω is the element of volume. This equation, originally devised by VINEN [16] in phenomenological considerations, was later developed by SCHWARZ [10]. Schwarz expressed original Vinen coefficients by $c_2(\alpha)$ and $I_l(\alpha)$, which describe the microscopic state of quantum tangle. He showed also by dynamical scaling that in the case of steady-state turbulence, these coefficients do not depend on L or V_{ns}.

2) Alternative Vinen equation (VINEN [16])

$$\frac{dL}{dt} = -\beta_{alt}\, L^2 + \alpha_{alt} L\, V_{ns}^2 \,, \tag{4.6}$$

where β_{alt} and α_{alt} are some new parameters.

First, we should note that the simplified Eq. (3.10) obtained in the proposed model strictly corresponds to the alternative Vinen equation. The generation term is proportional to LV_{ns}^2 what is closer to the phenomenological theory of classical turbulence (LANDAU, LIFSHITZ 1980). Indeed, (NIEMIROWSKI, FISZDON [6]) by assuming that turbulence can be characterized by a parameter, say, L, and that its time derivative dL/dt is an analytic function of L, the alternative form of Vinen equation can be interpreted as the first two terms of the series expansion. Furthermore, as the generation term is the scalar function of vector argument V_{ns}, it is reasonable that the series expansion starts with this argument squared. The last comment concerns also the complete form of the evolution equation obtained in the model, i.e. Eq. (3.7) where the counterflow velocity V_{ns} is also everywhere squared. The presence of absolute value of V_{ns} in the classical Vinen equation is rather strange.

Now we concentrate on the steady state turbulence and compare the equilibrium line-length densities L_∞ obtained in the model (Eq. (3.9)), in numerical simulations done by Schwarz (with the use of Vinen-Schwarz theory) and in real experiments. The equilibrium density obtained in our model is given by:

$$L_\infty = w(\alpha) \left(\frac{V_{ns}}{\beta} \right)^2 \,, \tag{4.7}$$

while in the Vinen-Schwarz theory

$$L_\infty = \left(\frac{I_l}{c_2^2} \right)^2 \left(\frac{V_{ns}}{\beta} \right)^2 = c_L^2 \left(\frac{V_{ns}}{\beta} \right)^2 \,. \tag{4.8}$$

As the dependence on V_{ns} is the same (as we noted in the introduction L_∞ must be proportional to V_{ns}), we have only to compare our function $w(\alpha)$ with

Schwarz's $c_L^2(\alpha) = \left(I_l/c_2^2\right)^2$, and with experimental results. Because the line-length density is measured indirectly by measuring the mutual friction force, we have to remind some facts. The normal fluid component exerts a force on the quantized vortices of the vortex tangle, and on the other hand, superfluid interacts with vortices by the Magnus force. In the result the vortices give rise to the friction force F_{ns} between the two components

$$F_{ns} = \rho_s \kappa \alpha I_m L V_{ns} \,, \tag{4.9}$$

where $I_m(\alpha)$ is another anisotropy coefficient, characterizing the vortex tangle. When the tangle is isotropic $I_m = 2/3$, but usually it varies between $2/3$ and 1. Schwarz found that it can be expressed as $I_m = I_{||} - c_L I_l$, where

$$I_{||} = \frac{1}{\Omega L} \int (1 - (s' \cdot \hat{V}_{ns})^2) d\xi \tag{4.10}$$

is the other directional anisotropy coefficient, and calculated it in his simulations. Because we cannot simply calculate $I_{||}$ in our model, to compare the results we take I_m from the Schwarz simulation.

Putting L from Eq. (4.8) or from Eq. (4.7) to Eq. (4.8), one gets:

$$F_{ns} = \frac{\rho_s \kappa \alpha}{\beta^2} f_\alpha V_{ns}^3 \,, \tag{4.11}$$

where the coefficient $f_\alpha = c_L^2 I_m$ in the Vinen-Schwarz theory or $f_\alpha = w I_m$ in the proposed model. The force F_{ns} can be determined in the counterflow experiments by measuring the temperature gradient

$$F_{ns} = \rho S \nabla T \,, \tag{4.12}$$

where S is the entropy per unit mass.

The coefficient f_α was used by SCHWARZ[10] and later by SCHWARZ and ROZEN [11] to compare the numerical results with experiments. In Fig. 3 we compare our results with Schwarz predictions and some experimental results chosen by Schwarz. Besides in Table 1 we present some coefficients characterizing quantum turbulence. From Fig. 3 one can see that the experimental results vary significantly from one experiment to another. For the same α the coefficient $f_\alpha^{1/3}$ vary by $20 - 40\%$, when considering various experiments; this gives the uncertainty of L of the order of 2. This is because the experiments are still not a good test for the model proposed here, or for the Schwarz theory. We may notice however, that our theoretical curve fits relatively better the recent SCHWARZ and ROZEN [11] experiment than the Schwarz theoretical curve.

Now we concentrate on non-equilibrium turbulence. Because even the measurements of steady state turbulence give very different results, comparing our

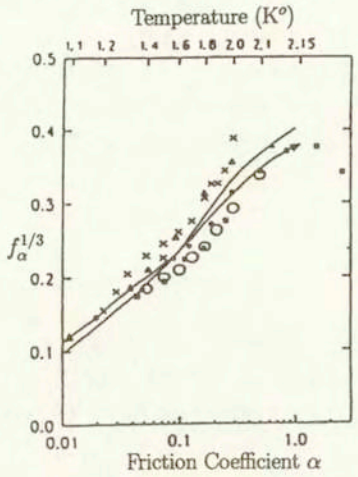

FIG. 3. The α dependence of the friction coefficient $(f_\alpha)^{1/3}$. The line ending with arrows – model predictions (3.9), second line – SCHWARZ [10] predictions basing on numerical simulations. Crosses represent pure superflow in 0.0057 cm by 0.057 cm channel (OPATOWSKI and TOUGH [8]), dots represent counterflow in 0.0366 cm capillary (BREWER and EDWARDS [2]), triangles are counterflow in a 0.240 by 0.645 cm channel (VINEN [14, 15, 17, 17]) squares represent counterflow in a 1.0 by 1.0 cm channel (SWANSON [12], SWANSON and DONNELLY [13]), and open circles are counterflow in 1.00 by 2.32 cm channel (SCHWARZ and ROZEN [11]).

evolution equation with experiments seems to be not useful. SCHWARZ and ROZEN found that the Vinen equation can fit satisfactorily their experimental curves, however the fitted coefficients I_l and c_L differ substantially from the calculated ones. In Fig. 4 we fit our evolution equation to Vinen evolution equation (with coefficients used by SCHWARZ and ROZEN to fit their experiments). Those two curves lie so close to each other that until we have no better experiments, we can not judge from them which form of evolution equation is better.

Table 1. Values of dimensionless parameters characterizing quantum turbulence. S – Schwarz simulation, M – proposed model.

Temp	1.07	1.26	1.62	2.01	2.15
ρ_n/ρ	0.013	0.039	0.174	0.576	0.886
α	0.010	0.030	0.100	0.300	1.00
$I_{\|\|} - c_L I_I$	0.70	0.72	0.71	0.77	0.85
w_α [M]	0.0022	0.0070	0.019	0.041	0.061
$c_L \sim w_\alpha$ [S]	0.0013	0.0053	0.019	0.0484	0.076
$\overline{f}_\alpha^{1/3}$ [M]	0.115	0.171	0.238	0.317	0.374
$f_\alpha^{1/3}$ [S]	0.097	0.156	0.238	0.334	0.401

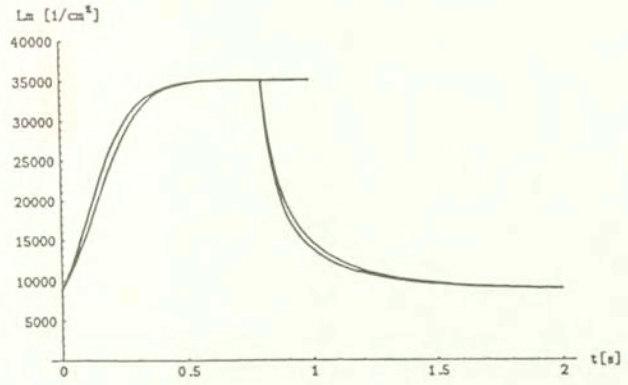

FIG. 4. The evolution of line-length density during the growth and decasy transient. At $t = 0$ the counterflow velocity is switched from $V_{ns} = 1$ cm/s to 2 cm/s, than at $t = 0.8$ s it is switched again to 1 cm/s. The "inner" line is a prediction of the Vinen equation with coefficients $c_{lm} = 0.0937$ and $I_{lm} = 0.65$ used by Schwarz to fit his experiments with Rozen. The "outer" line is the solution of our Eq. (3.7) with $A = 0.86$, $B = 0.137$.

Instead of comparing the theoretical predictions of our model with experiments, we propose to compare them with SCHWARZ [10] and SCHWARZ and ROZEN [11] simulations. In the paper [10] SCHWARZ assumed that the coefficient I_l and c_2 depend neither on L nor on V_{ns} and calculated them in the numerical simulations for equilibrium turbulence. Later, in the paper [11] SCHWARZ and ROZEN analyzed, by numerical simulations, large transients when the line-length density grows from very small to very large value, and concluded that $I_l = I_l(tL_\infty, L_i/L_\infty)$ and $c_2 = c_2(tL_\infty, L_i/L_\infty)$ where L_i is the initial value of line-length density. That conclusion written in a rather curious form (curious because it can not be simply applied e.g. to the case when V_{ns} varies harmonically) means in fact that I_l and c_2 depend on L and V_{ns}. This means that the classical Vinen equation is improper. Especially, as they found, the coefficient I_l which measured the anisotropy of the distribution of the binormal to the tangle varied significantly. In the simulations with $T = 1.6$ K i.e. $\alpha = 0.1$, the sudden change of counterflow V_{ns} by factor 3 causes a sharp change of I_l by roughly 50% (see Fig. 5). This phenomenon can be interpreted in our model; as we noted, the anisotropy results from the action of the counterflow between two subsequent reconnections, so it is clear that for the same line-length density the anisotropy will be larger for larger V_{ns}. Moreover we can calculate the anisotropy coefficient I_l from our model, by comparing the growth term of our evolution equation with the Vinen one. As the result we get:

$$\tilde{I}_l = B\alpha^{1/2}\,\beta^{-1/2}\,|V_{ns}|\,L^{-1/4}\,V_o^{-1/2}\,. \tag{4.13}$$

First, we notice that for steady-state turbulence ($L = L_\infty$)

$$\tilde{I}_{l\infty} = B\alpha^{1/2} \left(w_\alpha \left((1+\alpha^2) w_\alpha + \frac{2}{3}\alpha^2 \right) \right)^{-1/4} . \tag{4.14}$$

For $\alpha = 0.1$ we get $\tilde{I}_{l\infty} = 0.55$, while Schwarz obtained $I_{l\infty} = 0.45$ as asymptotic value for steady state turbulence. During the transition I_l varies. To conpare the dependence of I_l on scaled time $t_{sc} = \beta t L_\infty$ with Schwarz numerical results, we multiply our I_l by 0.45/0.55 to have the same asymptotic value; such difference of order 20% in asymptotic values is rather meaningless. The result is shown in Fig. 5. The coefficient $\tilde{c}_2^2$ corresponding to c_2^2 can be calculated by comparing the decaying terms in both equations:

$$\tilde{c}_2^2 = A\alpha^{-1/2}\, \beta^{-1/2}\, L^{-1/4}\, V_o^{1/2}; \tag{4.15}$$

its asymptotic value (for $L = L_\infty$) $c_{2\infty}^2$ is

$$\tilde{c}_{2\infty}^2 = A\alpha^{-1/2} \left(1 + \alpha^2 + \frac{2\alpha^2}{3w_\alpha} \right)^{1/4} . \tag{4.16}$$

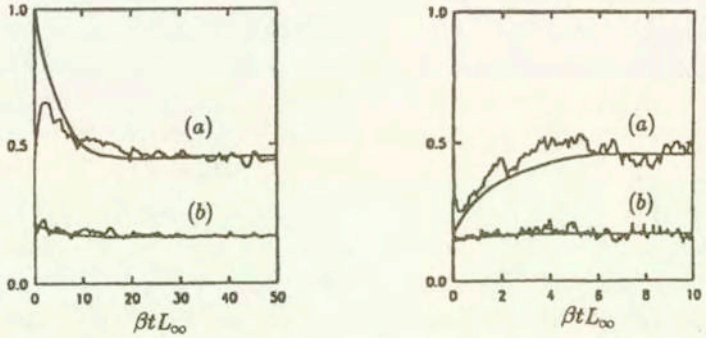

FIG. 5. The evolution of coefficients (a) – I_l and (b) – $c_2^2/20$ and the corresponding coefficient $\bar{I}_l$ and $\bar{c}_2^2/20$ during the growth (left) and the decay (right) transient. The smooth lines are the coefficients $\bar{I}_l$ and $\bar{c}_2^2/20$. In the growth transient the counterflow velocity V_{ns} is suddenly increased from V_o to $3V_o$, while in the decay transient it is decreased from V_o to $V_o/3$.

For $\alpha = 0.1$ we get $\tilde{c}_{\infty 2}^2 = 4.00$ while the Schwarz numerical value is $c_2^2 = 3.31$. Again, to compare our result with those of Schwarz, we rescaled our $\tilde{c}_2^2$ to have the same asymptotic value. From Fig. 5 we see the time dependence of our coefficient $\tilde{I}_l$ and $\tilde{c}_2^2$ corresponds somehow to the time dependence of Schwarz coeficients I_l and c_2^2. This means that our dynamic equation corresponds better to Schwarz simulations than to Vinen equation with constant coefficients. Our coefficients

$\tilde{I}_l$, $\tilde{c}_2^2$ depend only on L and V_{ns}, but in reality, some time after V_{ns} is switched, it is needed to change them. The reaction time in which the coefficients change is roughly equal to the characteristic time between the reconnections (Eq. (2.17))

$$t_c = \frac{1}{(\beta L)^{1/2} V_o} \,. \tag{4.17}$$

For the steady state turbulence for $\alpha = 0.1$ one gets $t_c = 0.86/\beta L$. This corresponds to the scaled time $t_{sc} = \beta t L_\infty$; $t_{sc} = 8$ in the beginning of growth transient, $t_{sc} = 0.1$ in the beginning of decay transient. This roughly agrees with the reaction time which can be deduced from Fig. 5. During the reaction time, the coefficients $\tilde{I}_l$ and $\tilde{c}_2^2$ cannot agree with those measured in the simulations. To determine the behavior of $\tilde{I}_l$ and $\tilde{c}_2^2$ during the reaction time, the separate equations are needed to supplement the evolution equation for line-length density.

5. Conclusions and perspectives

The main result of this work is the construction of the simple model in which the microscopic analysis of quantum tangle leads to macroscopic evolution equation for line-length density. The numerical simulations needed to estimate coefficients A, B in Eq. (3.7) are relatively simple and not time-consuming, when compared with the simulations of Schwarz. The main advantage of the presented approach is the possibility of generalizing it to anisotropic flows with significant macroscopic superfluid vorticity. Such flows are expected in such phenomena as spin-up or boundary layer forming. The viscous forces in a cylinder, which start spinning from the rest, acting on normal component, may give rise to the counterflow, large enough to cause the quantum turbulence which may significantly influence the dynamics of both components. In this way the angular momentum can be transferred from the cylinder via the normal component to the superfluid component. One may expect the following scenario: due to viscous forces, the normal component starts spinning, and this implies counterflow which generates quantum turbulence. The mutual friction forces couple the two components ($V_{ns} \to 0$) and in the end, the quantum vortices polarize to form a pattern of straight parallel lines and both fluids spin together. However, because of the large normal fluid velocity gradients, even in first stages of spin-up process the arising quantum turbulence is highly anisotropic; the tangle of quantized vortices is polarized to carry considerable macroscopic superfluid vorticity. This is probably why the description of spin-up process in terms of the Vinen model was found to be inconsistent (LIPNIACKI [3]). The line-length density calculated from Vinen equation was smaller then the line density calculated from superfluid velocity profiles. The origin of these vortices cannot be explained within the Vinen model.

To analyze the superfluid turbulent flows with net vorticity, the generalization of the model for an anisotropic turbulence is needed.

Macroscopic vorticity introduces into quantum turbulence an additional anisotropy parameter q.

$$q = \frac{\omega_s}{\kappa L} = \frac{L_{\|}}{L} = \frac{\int s' \cdot \hat{z} d\xi}{\int d\xi} , \tag{5.1}$$

where $L_{\|} = \omega_s/\kappa$ is the minimal vortex line-density needed to generate superfluid vorticity ω_s, $\hat{z}$ is unit vector parallel to the z axis, and s' (recall) is the unit vector tangent to vortex line $s(\xi, \tau)$. The parameter $q \in [0, 1]$; $q = 0$ corresponds to the isotropic case, while $q = 1$ corresponds to the system of straight parallel vortex lines.

The anisotropy influences significantly the evolution of the tangle, and at least three aspects must be taken in to account:

1) The non-zero macroscopic superfluid vorticity ω_s influences the superfluid flow. Hence to calculate the counterflow V_{ns} the superfluid macroscopic velocity V_s must be calculated from macroscopic ω_s by the Biot-Savart law. Another way will be to calculate the superfluid vortex velocities directly from the Biot-Savart law basing on positions of all vortices (see BARENGHI *et al.* [1]) but this method is numerically very expensive and can be applied only to relatively rarefied vortex tangle.

2) For $q > 0$ the vortex lines prefer to lie along one direction, so the average relative angle between vortex lines is smaller than in the isotropic case. This implies that average collision surface $\sigma(q)$ and reconnection frequency f_{rq} are smaller than σ_o and f_r, respectively. Because the reconnection frequency is proportional to the collision surface (Eq. (2.13), (2.15)), we may express f_{rq} as follows:

$$f_{qr} = \frac{\sigma(q)}{\sigma_o} f_r = \frac{\sigma(q)}{\sigma_o} \, l_o \, v_o \, L , \tag{5.2}$$

where $\sigma_o = \pi/4$ and $f_r = l_o \, v_o \, L$ correspond to the isotropic case, and $\sigma(q)$ has to be calculated.

3) The average relative angle between reconnecting lines will be smaller, hence the average line-length change $\Delta S_o(q)$ due to each reconnection will be different. $\Delta S_o(q)$ may be expressed in the same form as in Eq. (3.4)

$$\Delta S_o(q, \tau) = -a(q) \, (\alpha\tau)^{1/2} + b(q) \, (\alpha\tau)^{3/2} v_{ns}^2 , \tag{5.3}$$

but with coefficients $a(q)$, $b(q)$ instead a_o, b_o.

Acknowledgments

The author is grateful to Professor Peradzyński for stimulating discussion and comments. This work was supported by the KBN grant 7T07A 01817.

References

1. C. F. BARENGHI, G. H. BAUER, R. J. DONNELLY, D. C. SAMUELS, *Superfluid vortex lines in a model of turbulent flow*, Phys. Fluids, **9**, 9, 2631–2643, 1997.
2. B. F. BREWER, D. O. EDWARDS, *Heat Conduction by liquid helium II in capillary tubes III mutual friction*, Philos. Mag., **7**, 721–735, 1962.
3. T. LIPNIACKI, *Dynamics of superfluid Helium – limits of the Vinen model*, Arch. Mech., **49**, 4, 615–633, 1997.
4. T. LIPNIACKI, *Dynamics of quantum vortices in superfluid ^{4}He*, Arch. Mech., **50**, 3, 467–482, 1998.
5. T. LIPNIACKI, *Evolution of quantum vortices following reconnection*, Eur. J. Mech., B/Fluids, **19**, 361–378, 2000.
6. S. K. NEMIROWSKI, W. FISZDON, *Chaotic quantized vortices and hydrodynamic processes in superfluid helium*, Rev. Mod. Phys., **67**, 1, 37–84, 1995.
7. C. NORE, M. ABID, M. E. BRACHET, *Decaying Kolmogorov turbulence in a model of superflow*, Phys. Fluids, **9**, 9, 2644–2669, 1997.
8. L. B. OPATOWSKY, J. T. TOUGH, *Homogeneity of turbulence in pure superflow*, Phys. Rev., **B 24**, 5420–5421, 1981.
9. K. W. SCHWARZ, *Three-dimensional vortex dynamics in superfluid ^{4}He: Line-line and line-boundary interactions*, Phys. Rev., **B 31**, 5782–5804, 1984.
10. K. W. SCHWARZ, *Three-dimensional vortex dynamics in superfluid ^{4}He: Homogenous superfluid turbulence*, Phys. Rev., **B 38**, 2398–2417, 1988.
11. K. W. SCHWARZ, J. R. ROSEN, *Transient behavior of superfluid turbulence in a large channel*, Phys. Rev., **B 44**, 7563–7577, 1991.
12. C. E. SWANSON, *A study of vortex dynamics in counterflowing helium II*, Ph. D. thesis, University of Oregon, 1985.
13. C. E. SWANSON, R. J. DONNELLY, *Vortex dynamics in turbulent counterflowing helium II*, J. Low Temp. Phys., **61**, 363–399, 1985.
14. W. F. VINEN, *Mutual friction in heat current in liquid helium II, I, Experiments on Steady Currents*, Proc. R. Soc. London, Ser. A **240**, 114–127, 1957a.
15. W. F. VINEN, *Mutual friction in heat current in liquid helium II, II, Experiments on transient effects*, Proc. R. Soc. London, Ser. A **240**, 128–143, 1957b.
16. W. F. VINEN, *Mutual friction in heat current in liquid helium II, III. Theory of the mutual friction*, Proc. R. Soc. London, Ser. A **242**, 493–515, 1957c.
17. W. F. VINEN, *Mutual friction in heat current in liquid helium II, IV. Critical heat currents in wide channels*, Proc. R. Soc. London, Ser. A **243**, 400–413, 1958.

Received August 30, 2000; revised version November 27, 2000.